Supporting Information

Electrolyte Membranes with Biomimetic Lithium-Ion Channels

Wenyue Shi,[§‡] Jianqiang Shen,[§‡] Li Shen,[§] Wei Hu,[⌀] Pengcheng Xu,[§] Jesse A. Baucom,[§] Shengxiang Ma,[§] Shuxing Yang,[§] Xiao-Ming Chen[||] and Yunfeng Lu[§]**

[§]Department of Chemical and Biomolecular Engineering, University of California, Los Angeles, CA 90095, USA

[⌀]College of Chemistry, Northeast Normal University, 5268 Renmin Street, Changchun 130024, PR China

[||]School of Chemistry and Chemical Engineering, Sun Yat-Sen University, Guangzhou 510275, PR China

‡ Wenyue Shi and Jianqiang Shen contribute equally to this work.

E-mail address: lishen@ucla.edu, luucla@ucla.edu

Methods

Synthesis of UN-SLi. UN was synthesized according to reported literature through a hydrothermal reaction.[1] As-synthesized UN was mixed with excess 1,3-propanesultone in $CHCl_3$. After stirring at 45 °C for 12 h, the bright yellow solid was collected through centrifugation. The solid was washed by $CHCl_3$ three times then dried at 80 °C to obtain UN-SH. UN-SLi was prepared by reacting UN-SH with excess LiCl aqueous solution. The final UN-SLi was collected by filtering,

washed by water and ethanol for three times each, and dried at 120 °C under vacuum for complete removal of water.

Preparation of REF and UN-SLi-EM. UN-SLi-EM was prepared by homogenously mixing 480 mg of MOFs (UN-SLi) with 320 mg of P(VdF-HFP) powders in 10 mL of dimethyl carbonate (DMC) and 2 mL of ethylene carbonate (EC) for 24 h (ambient temperature). 150 μL of resulting suspension was uniformly added to each side (300 μL in total) of a glass-fiber separator (18.5 mm in diameter, Whatman, GF/C). REF was prepared by a similar process without MOFs. After evaporation of DMC solvents, all membranes were stored in glove box for future characterizations and hot-pressed before being used.

Approximation of the Debye length of sulfonate groups. Assuming the lithium sulfonate groups ionize completely in the EC/DEC solvents, the following formula of Debye length for symmetric monovalent electrolytes is used for the calculation: $\lambda_D=(\varepsilon_r\varepsilon_0 k_B T/q^2\Sigma z_i^2(N_A c_i))^{1/2}$ [2,3] (1), where λ_D is the Debye length in electrolyte solutions, ε_r is the relative dielectric constant of the solvent, $\varepsilon_0 = 8.85\times10^{-12}$ F·m^{-1} is the vacuum permittivity, $k_B = 1.38\times10^{-23}$ J K^{-1} is the Boltzmann constant, T is the absolute temperature in kelvin, $q = 1.60\times10^{-19}$ C is the elementary charge, z_i is the charge number of the ion, $N_A = 6.02\times10^{23}$ mol^{-1} is the Avogadro constant, and c_i is the molar concentration of the ion in the electrolyte (mol L^{-1}). At T = 298 K (25 °C), ε_r for DEC is 2.82, while EC alone has a melting point higher than T = 298 K. Therefore, $\varepsilon_r = 90.36$ at T = 313 K for EC is used as an approximation.[4] The dielectric constant for the mixed EC/DEC solvents is considered roughly linear[5], thus $\varepsilon_r = 46.59$ can be estimated for the EC/DEC solvents (volume ratio 1:1). Considering the chemical formula of UN-SLi ($Zr_6O_{38.3}C_{54.3}H_{44.5}N_6S_{2.1}Li_{2.1}$) and the available liquid electrolyte in UN-SLi-EM (12 mg of UN-SLi in 160 μL of electrolyte), a molar

concentration of the negatively charged sulfonate residues can be calculated as 7.8×10^{-2} mol L^{-1}. Taking all the derived numbers into formula (1), a Debye length of $\lambda_D = 8.4$ Å can be approximated.

Electrochemical studies. All electrochemical characterizations were carried out by adding an equivalent amount of liquid electrolyte (160 μL of 1M $LiPF_6$ in EC/DEC with 5 wt% FEC) to the membranes studied (UN-SLi-EM, REF). CV tests (Biologic VMP3) were conducted in coin-cell configuration with a scan rate of 1.0 mV s^{-1} between –0.2 and 5.0 V, where lithium chips were utilized as reference/counter electrodes and stainless-steel plates were used as the working electrodes.

The ionic conductivity (σ, S cm^{-1}) was measured by sandwiching electrolyte-saturated membranes by two blocking electrodes (stainless steel plates) and calculated based on the following equation: $\sigma=4L/\pi RD^2$, where σ is conductivity, L (cm) and D (cm) are thickness and diameter of the membranes, respectively, and R (Ohm) is the resistance obtained from EIS (Solartron 1860/1287) by AC amplitude of 10 mV from 10^6 to 1 Hz. The ionic conductivity of UN-SLi was measured in a similar manner using a densified pellet (25 kpsi) made by sulfonated MOF powders and organic solvents (33 wt%).[6]

Determination of t_{Li^+} was performed through the combined measurement of alternating-current (AC) impedance and potentiostatic polarization. The time dependence of the current was detected via Li|Li symmetric cell with a voltage of 20 mV (ΔV) applied, during which the initial current (I_0) was monitored until reaching the steady-state current (I_{ss}). The same cell was monitored to measure the resistance of the electrolyte and the electrolyte–Li metal interface by EIS before (R_0) and after (R_{ss}) (10^6 to 1 Hz, 10 mV amplitude) applying the voltage. t_{Li^+} can be calculated with the following expression: $t_{Li^+} = I_{ss}(\Delta V - I_0R_0)/ I_0(\Delta V - I_{ss}R_{ss})$.[7]

Li stripping and plating tests were performed using Li|Li cells by galvanostatically charging and discharging (Landt instrument) for a period of 2 h each at a current density of 1.0 mA cm^{-2}, except for initial 10 cycles at 0.2 mA cm^{-2}. The post-mortem evaluations on Li electrodes and UN-SLi-EM membranes were carried out by dissembling Li|Li cell after 50 cycles (200 h). Cu|Li asymmetric cells were assembled by a lithium chip and copper foil (15 μm in thickness) in a coin cell. Each cycle includes plating lithium on the copper with a current density of 1.0 mA cm^{-2} for 2 h and stripping to voltage cutoff at 1.0 V (*vs*. Li/Li^+).

Prototype batteries were fabricated by assembling a conventional $LiFePO_4$ cathode (2/13 mg cm^{-2}) and a Li anode (760/50 μm) in coin cells (2.5 to 4 V *vs*. Li/Li^+ for $LiFePO_4$). The $LiFePO_4$ cathodes were prepared by homogenously blending $LiFePO_4$ (MTI), acetylene black, and polyvinylidene difluoride (PVdF) at a ratio of 8:1:1 in N-Methyl-2-pyrrolidone (NMP). The resulting slurry was uniformly coated on a conductive carbon-coated Al foil and dried in a vacuum oven at 90 °C for 12 h. The specific capacity is calculated based on the active materials in the cathode. 1C charging and discharging rate here is defined as 150 mA g^{-1}. All the electrochemical tests were carried out at ambient temperature (≈ 25 °C) unless specified.

Materials characterizations and structural analysis. Crystalline structures of MOFs samples were determined by the Rigaku powder X-ray diffractometer (XRD) using Kα radiation (λ = 1.54 Å). Surface morphology and particle sizes were investigated by scanning electron microscopy (Nova 230 Nano SEM) and transmission electron microscopy (FEI T12 Quick CryoEM and CryoET TEM). N_2 sorption/desorption measurements were conducted using a Micromeritics ASAP 2020 system at 77 K. Prior to the measurement, all samples were degassed at 120 °C for 12 h. All ^1H NMR samples were prepared by completely digesting MOFs samples (6 mg) in 30 μL 48% HF solution and 570 μL DMSO-d6. After sonication, MOF particles were completely

dissolved, and further analyzed by AV400 NMR (auto-sampler). AV400 was used with 5 mm broadband with Z gradient. Inductively coupled plasma atomic emission spectroscopy (ICP-AES) was performed using Shimadzu ICP-9000 instrument. The UN-SLi was digested by excessive concentrated HNO_3 and HCl (vol. 1:3), dried to remove the liquid, dissolved in 5% HCl solution and formed diluted solution for the ICP-AES test. The standard curves were obtained by measuring Li^+ and Zr^{4+} standard solutions with the concentrations of 0, 5, 10, 25, 50 ppm. X-ray photoelectron spectroscopy (XPS) measurements were performed on an AXIS Ultra DLD instrument. The samples were prepared in glovebox before quickly transferred to a high-vacuum chamber. The obtained raw XPS spectra were calibrated by C 1s peak at 284.8 eV and then fitted based on Gaussian−Lorentzian functions and Shirley-type background. Raman spectroscopy was conducted on a Renishaw 2000 System with a He/Ne laser at a wavelength of 633 nm. Zeta potential was measured on Zetasizer Nano instrument (Malvern) with isopropanol as the solvent. A home-made permeation cell was made by sandwiching UN-SLi-EM or REF between two cells. The left one contains anionic dye G250 (Coomassie brilliant blue) in methanol (5 mg L^{-1}) and the right left contains pure methanol with same volume. The pictures were taken in chronological order to allow dye molecules diffuse from left to right cells.

COMSOL Multiphysics Simulation. The model includes following processes: (1) charge transport: electronic charge transport in electrodes, and ionic charge transport in electrolyte; (2) species transport: in electrolyte, and within particles of electrodes; (3) Butler-Volmer electrochemical kinetics for electrodes.[10] As for domains, the model uses: (1) liquid electrolyte (1M $LiPF_6$ salt in carbonate solvents) in porous separator; (2) positive porous electrode ($LiFePO_4$ particles as active material), partial physical properties are obtained from manufacturer datasheet; (3) at negative electrode, lithium foil is used as planar electrode. As for boundary conditions, (1)

on the current collector/active material boundaries, for electronic current balance, electric potential is set 0 V at the negative electrode, and current density is given by applied discharge rate at the positive electrode; (2) current collector/active material boundaries are insulating for ionic charge balance; (3) at particle surfaces in electrodes, the species flux is determined by Butler-Volmer equation (reaction rates of electrochemical reactions).[11]

Supporting Figures

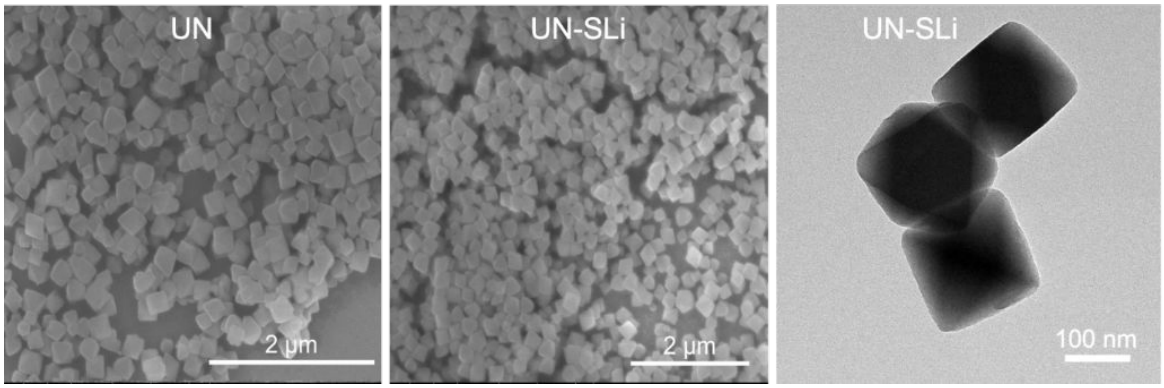

Figure S1. SEM images of (a) as-synthesized UN and (b) UN-SLi. (c) TEM image of UN-SLi.

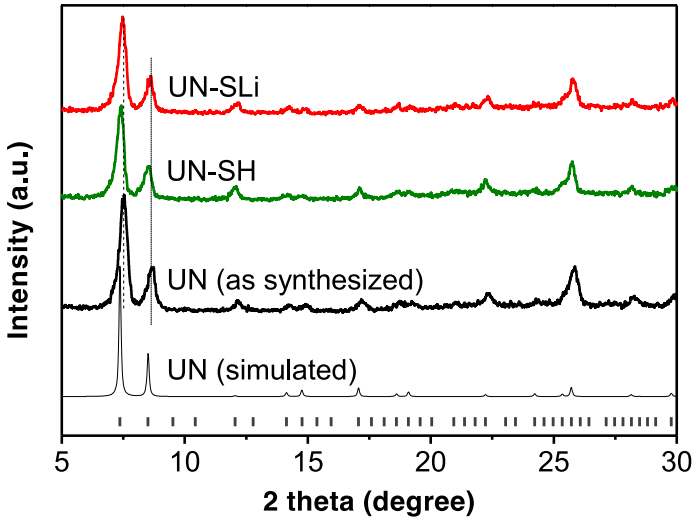

Figure S2. XRD patterns of UN, UN-SH and UN-SLi. A simulated UN pattern is also plotted at the bottom.

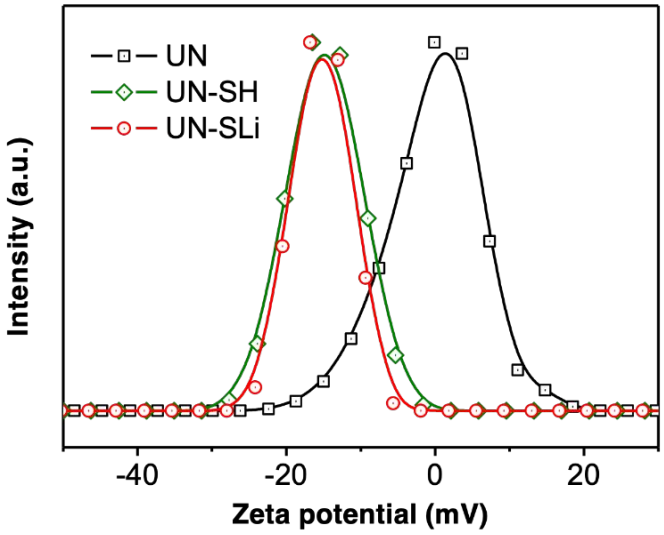

Figure S3. Zeta potential measurements of UN, UN-SH and UN-SLi in organic medium (isopropanol).

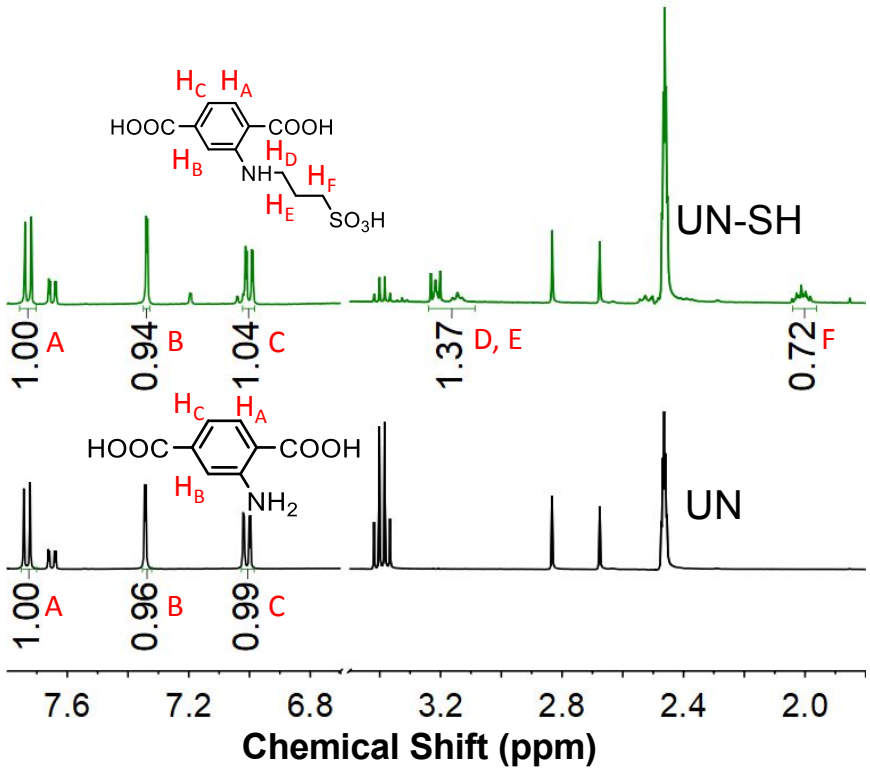

Figure S4. ^{1}H NMR spectra of UN and UN-SH (3.8-6.6 ppm is omitted).

Table S1. ICP-AES measurement for UN-SLi.

Element	weight concentration (mg L^{-1})	molar concentration (mmol L^{-1})	molar ratio (Li/Zr)
Zr	19.2	0.21	35.5%
Li	0.517	0.0745	

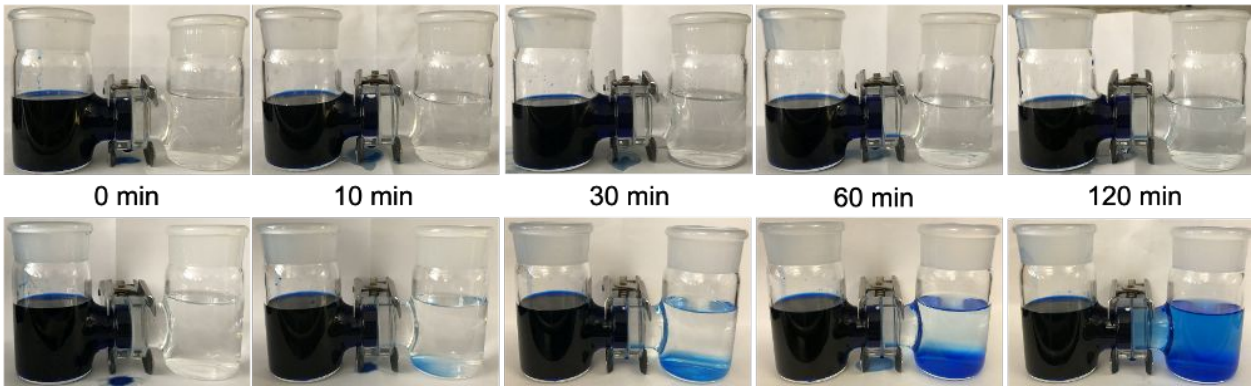

Figure S5. Anionic dye (G250) permeation experiments using UN-SLi-EM (upper) and REF (bottom).

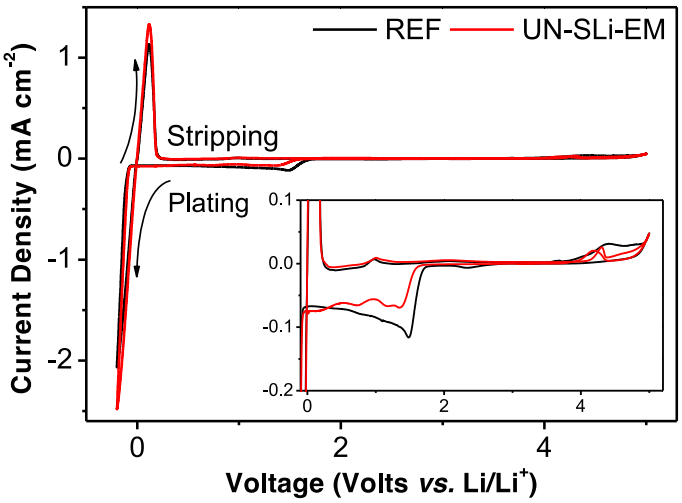

Figure S6. CV curves of liquid electrolytes in REF and UN-SLi-EM using stainless steel as working electrode and Li as counter/reference electrodes (inset shows the enlarged view).

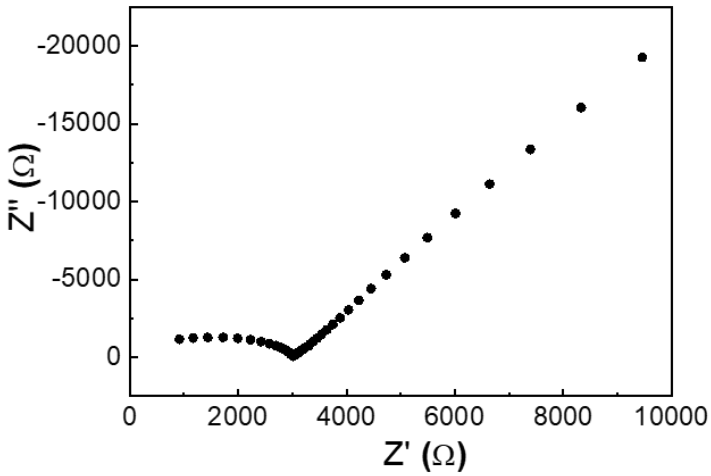

Figure S7. Nyquist plots of UN-SLi pellet wetted by solvents (~ 20 ºC). Note: the ionic resistance was derived from the intercept of semicircle and straight line.

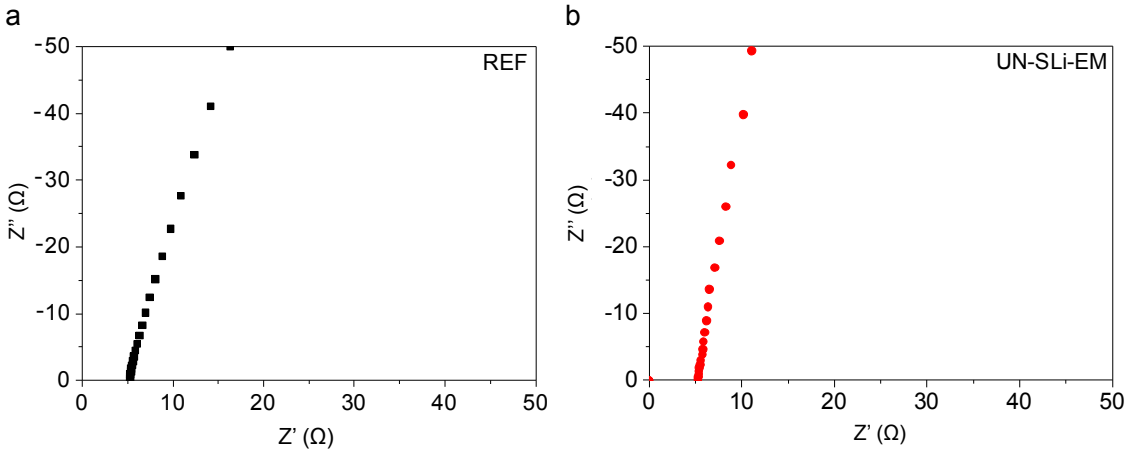

Figure S8. Nyquist plots (~ 20 ºC) of (a) REF and (b) UN-SLi-EM with equivalent amount of liquid electrolyte (160 µL of 1M $LiPF_6$ in EC/DEC). Note: the ionic resistance was derived from the intercept of the plots with real axis.

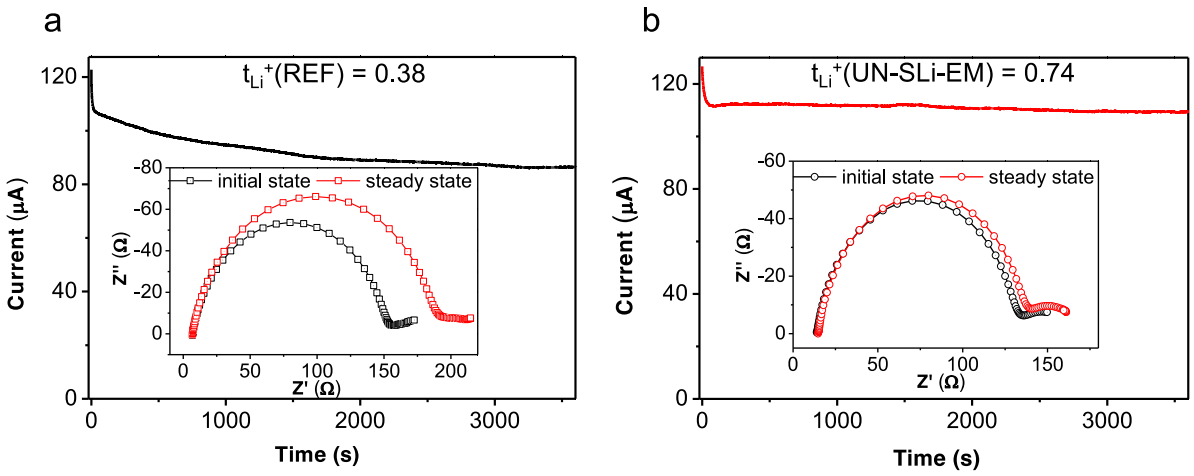

Figure S9. t_{Li}^+ measurements of liquid electrolytes in (a) REF and (b) UN-SLi-EM using potentiostatic polarization (insets: Nyquist plots before and after polarization).

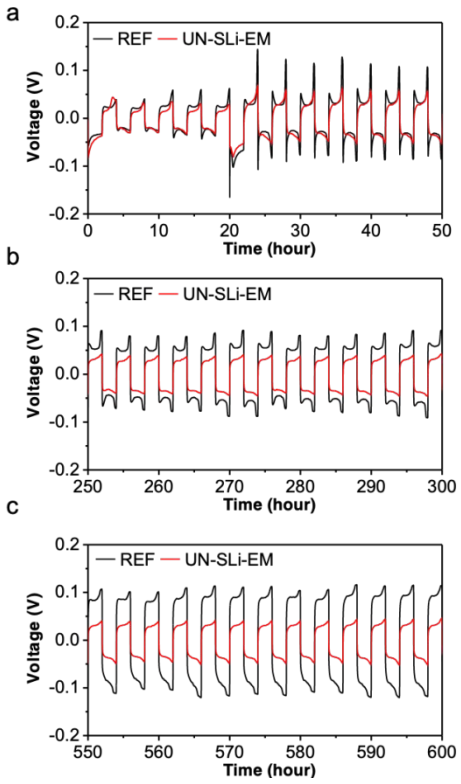

Figure S10. Enlarged time-dependent voltage profiles from the Li|Li cells at segments of (a) 0-50 h, (b) 250-300 h, and (c) 550-600 h. Areal capacity of 0.5 mAh cm^{-2} at 0.25 mA cm^{-2} for the initial 20 h and 2.0 mAh cm^{-2} at 1.0 mA cm^{-2} for cycles afterwards.

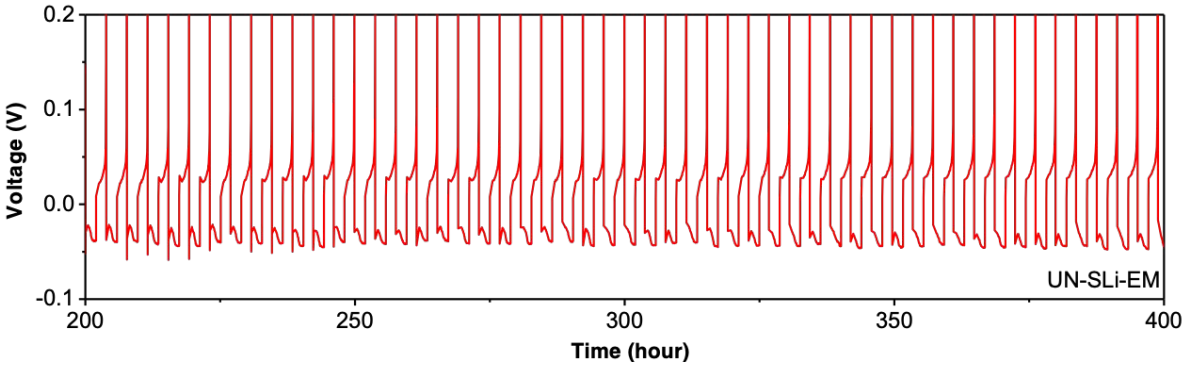

Figure S11. Time-dependent voltage profile (between 50th to 100th cycle) of Cu|Li cell using UN-SLi-EM.

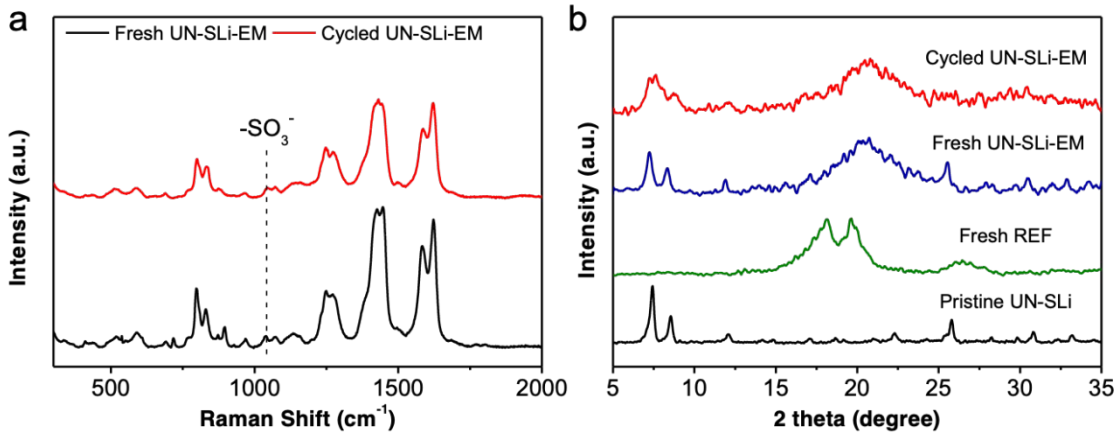

Figure S12. Post-cycle evaluations on UN-SLi-EM harvested from Li|Li cycling. (a) Raman spectrum of UN-SLi-EM comparing the fresh UN-SLi-EM. (b) XRD pattern of fresh and cycled UN-SLi-EM compared to UN-SLi powder and fresh REF.

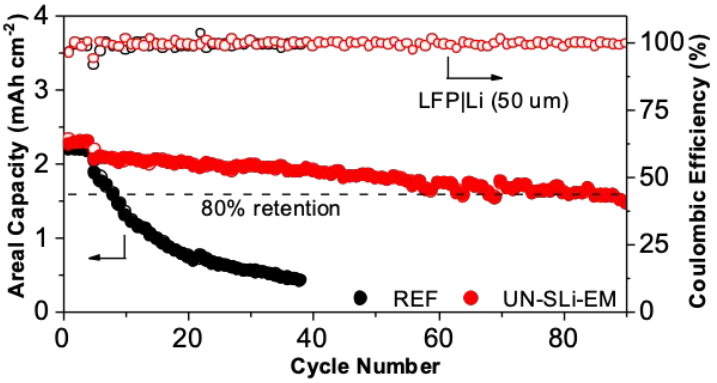

Figure S13. Galvanostatic cycling of LFP|Li (50μm) cells at 0.3 C (1 C = 150 mA g^{-1}).

Table S2. List of parameters (adapted from COMSOL manual "1D Isothermal Lithium-Ion Battery")[12,13]

Parameter	Value [Unit]	Meaning
i_1C	3 [A m^{-2}]	1C discharge current
C	1	Discharge rate
t_plus	0.38	Li-ion transference number (in non-separator region)
sigma_f	1	Scaling factor for electrolyte ionic conductivity (in non-separator region)
t_plus_SEP	0.38	Li-ion transference number (in separator region)
sigma_f_SEP	0.36	Scaling factor for electrolyte ionic conductivity (in separator region)
cl_0	1000[mol m^{-3}]	Initial electrolyte salt concentration
c_ref	1000[mol m^{-3}]	Reference electrolyte salt concentration for ionic conductivity interpolation
L_sep	140e-6[m]	Length of separator
L_pos	10e-6[m]	Length of positive electrode
T	298[K]	Temperature
rp_pos	2e-6[m]	Particle radius positive electrode
epsl_pos	0.63	Electrolyte phase volume fraction, positive electrode
epss_filler_pos	0.073	Conductive filler phase volume fraction, positive electrode
epss_pos	1-epsl_pos-epss_filler_pos	Electrode phase volume fraction, positive electrode
epss_neg	1-epsl_neg-epss_filler_neg	Solid phase vol-fraction negative electrode
csmax_neg	26390[mol m^{-3}]	Max solid phase concentration negative electrode
cs0_neg	26000[mol m^{-3}]	Initial concentration negative active electrode material
cs0_pos	3900[mol m^{-3}]	Initial concentration positive active electrode material
Ks_neg	100[S m^{-1}]	Solid phase conductivity negative electrode
k_pos	4.8e-10[m s^{-1}]	Reaction rate coefficient positive electrode
brugg	3.3	Bruggeman coefficient

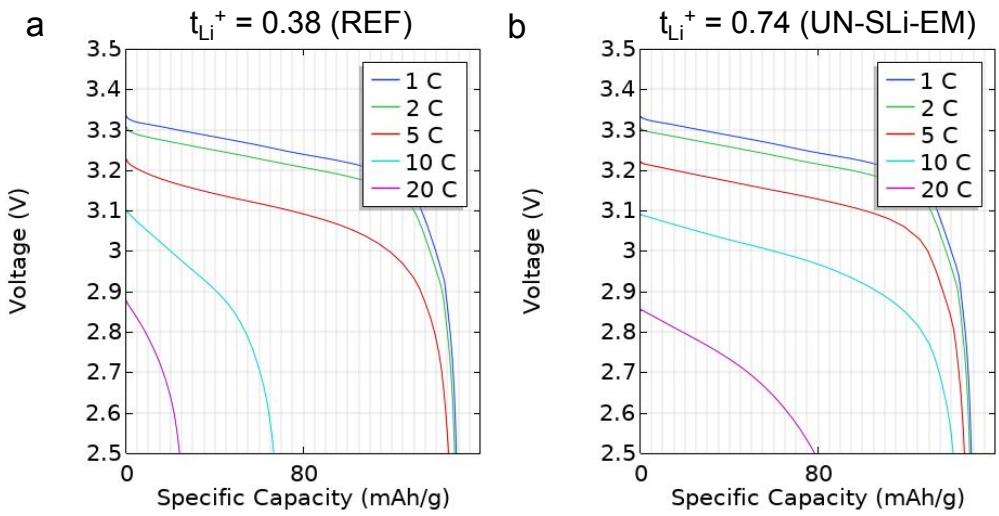

Figure S14. Output voltage profiles from simulated conceptual cell (LFP|Li) as a function of C-rate.

Supporting References:

(1) Katz, M. J.; Brown, Z. J.; Colón, Y. J.; Siu, P. W.; Scheidt, K. A.; Snurr, R. Q.; Hupp, J. T.; Farha, O. K. A Facile Synthesis of UiO-66, UiO-67 and Their Derivatives. *Chem. Commun.* **2013**, *49*, 9449–9451.

(2) Russel, W. B.; Saville, D. A.; Schowalter, W. R. *Colloidal Dispersions*; Cambridge University Press: Cambridge, 1989.

(3) Kohonen, M. M.; Karaman, M. E.; Pashley, R. M. Debye Length in Multivalent Electrolyte Solutions. *Langmuir* **2000**, *16*, 5749–5753.

(4) Wrodnigg, G. H.; Besenhard, J. O.; Winter, M. Cyclic and Acyclic Sulfites: New Solvents and Electrolyte Additives for Lithium Ion Batteries with Graphitic Anodes? *J. Power Sources* **2001**, *97–98*, 592–594.

(5) Jouyban, A.; Soltanpour, S.; Chan, H.-K. A Simple Relationship between Dielectric Constant of Mixed Solvents with Solvent Composition and Temperature. *Int. J. Pharm.* **2004**, *269*, 353–360.

(6) Peterson, G. W.; DeCoste, J. B.; Fatollahi-Fard, F.; Britt, D. K. Engineering UiO-66-NH_2 for Toxic Gas Removal. *Ind Eng Chem Res* **2014**, *53*, 701–707.

(7) Zugmann, S.; Fleischmann, M.; Amereller, M.; Gschwind, R. M.; Wiemhöfer, H. D.; Gores, H. J. Measurement of Transference Numbers for Lithium Ion Electrolytes via Four Different Methods, a Comparative Study. *Electrochim. Acta* **2011**, *56*, 3926–3933.

(8) Cai, G.; Jiang, H.-L. A Modulator-Induced Defect-Formation Strategy to Hierarchically Porous Metal-Organic Frameworks with High Stability. *Angew. Chem. Int. Ed. Engl.* **2017**, *56*, 563–567.

(9) Cai, G.; Ding, M.; Wu, Q.; Jiang, H.-L. Encapsulating Soluble Active Species into Hollow Crystalline Porous Capsules beyond Integration of Homogeneous and Heterogeneous Catalysis. *Natl Sci Rev* **2020**, *7*, 37–45.

(10) Lagadec, M. F.; Zahn, R.; Wood, V. Characterization and Performance Evaluation of Lithium-Ion Battery Separators. *Nat. Energy* **2018**.

(11) Lee, B.-S.; Yang, H.-S.; Jung, H.; Jeon, S.-Y.; Jung, C.; Kim, S.-W.; Bae, J.; Choong, C.-L.; Im, J.; Chung, U.-I.; *et al.* Novel Multi-Layered 1-D Nanostructure Exhibiting the Theoretical Capacity of Silicon for a Super-Enhanced Lithium-Ion Battery. *Nanoscale* **2014**, *6*, 5989–5998.

(12) Moura, S. J.; Argomedo, F. B.; Klein, R.; Mirtabatabaei, A.; Krstic, M. Battery State Estimation for a Single Particle Model with Electrolyte Dynamics. *IEEE Trans. Contr. Syst. Technol.* **2017**, *25*, 453–468.

(13) Cai, L.; White, R. E. Mathematical Modeling of a Lithium Ion Battery with Thermal Effects in COMSOL Inc. Multiphysics (MP) Software. *J. Power Sources* **2011**, *196*, 5985–5989.